

Statistical modeling of atmospheric turbulence based on a low-cost experimental setup for measuring C_n^2 over water

TAMARA S. CARVALHO,* CLAISSO P. AZZOLIN,  AIRTON F. GURGEL JR., 
VÍTOR G. A. CARNEIRO,  AND MARIA THERESA M. R. GIRALDI

Military Institute of Engineering, Rio de Janeiro, Brazil

*tamara.carvalho@ime.eb.br

Received 6 December 2022; revised 17 February 2023; accepted 20 February 2023; posted 24 February 2023; published 24 March 2023

The performance of communication systems based on free-space optical links depends on external factors such as weather conditions. Among many atmospheric factors, turbulence can be the greatest challenge to performance. The characterization of atmospheric turbulence usually involves expensive equipment known as a scintillometer. This work presents a low-cost experimental setup for measuring the refractive index structure constant over water, which results in a statistical model based on weather conditions. The turbulence variations with air and water temperature, relative humidity, pressure, dew point, and different watercourse widths are analyzed for the proposed scenario. © 2023 Optica Publishing Group

<https://doi.org/10.1364/JOSAA.482633>

1. INTRODUCTION

Most of the Amazon rainforest is in the Brazilian territory. This region, of great worldwide importance, is made up of several rivers and cities with a considerable number of inhabitants. As an example, São Gabriel da Cachoeira, a town located 852 km from the largest city in the region, Manaus, has a territory of 109,185 km² and 41,031 inhabitants [1].

In 2015, the Connected Amazon Program (in Portuguese, PAC—Programa Amazônia Conectada) was instituted [2], whose objective is to bring a fiber optic infrastructure to isolated cities located on the banks of the main rivers in the state of Amazonas, Brazil. To date, 1.9 thousand kilometers of fiber optic cables have been laid in the beds of the Solimões and Negro rivers and already serve the large municipalities in this region [3].

However, some small villages located close to the municipalities served by the PAC still suffer from a lack of high-quality data connections, as they are often separated from large municipalities by dense forests or small creeks, making wired connections unfeasible.

Faced with this scenario, the Brazilian Army, which is part of the PAC and responsible for building the entire underwater network infrastructure, felt the need to research viable solutions with high data transmission capacity.

Free-space optics (FSO) is a technology with the potential to provide high-rate communications. In addition, it also has other advantages over fiber or radio communications: the operating range does not require licenses, transmission is not

susceptible to interference from electromagnetic waves, there is no need to install pipelines or even underground installations, the instrumentation is relatively compact, and it has low power consumption [4]. Furthermore, the FSO does not face the difficulty of finding a free operating range within a crowded electromagnetic spectrum. Currently, commercial FSO systems are capable of transmitting data at a rate of up to 3 Gbps as long as there is a direct target [5]. However, recent studies predict rates of up to 400 Gbps [6]. With the advent of 5th generation (5G) and 6th generation (6G) technologies, FSO transmissions seem to have a very promising field of employment [7].

Although there are some point-to-point FSO solutions that achieve high data rates, such as 10 Gbps, this technology is still not used on a large scale. In addition to the considerable cost of acquiring such equipment, its performance is limited by external factors, such as base vibrations, rain, low visibility, winds, and sudden temperature changes, among other atmospheric factors [8]. Models for atmospheric attenuation are well known [9,10] and easy to incorporate into a link power budget, but dealing with atmospheric turbulence, which has a random nature, requires a statistical approach [11,12]. In a heterogeneous channel, such as in FSO links partially over water, it is extremely difficult to build an analytical model that describes atmospheric turbulence. The method proposed in this work considers heterogeneous links, i.e., links mounted partly over water and partly over ground. Some authors prefer to develop a more practical solution to estimate the received signal strength indicator (RSSI), based on empirical models built from meteorological measurements [13–15]. However,

this approach often ends up limiting the model to the conditions of the experiment.

It is also possible to develop an empirical model only for atmospheric turbulence [16]. In this case, the power balance can be performed by including terms already well modeled, such as geometric, atmospheric, and misalignment attenuation, plus an equivalent term that represents the attenuation caused by turbulence effects (mostly scintillation). The problem with this approach lies in the question of how to measure atmospheric turbulence. Many times, a scintillometer is used [17,18]. Unfortunately, this equipment has a very high cost, which makes it prohibitive for some researchers. The refractive index structure constant C_n^2 is the most used parameter for measuring atmospheric turbulence. There are several ways to obtain this parameter, such as the optical power triangulation method [19] or using ultrasonic anemometers [20,21] or electro-optical sensors [22].

This work aims to present a methodology for constructing a low-cost statistical model to measure atmospheric turbulence, using the relationship between C_n^2 and the temperature structure constant C_T^2 expressed in [11]. As a proof of concept for the method, we developed a statistical model for a scenario where an FSO link is established in a route partially over land and partially over water. This scenario was inspired by the Amazon region, where several cities were established on the banks of large rivers. The proposed methodology can be used in any region to model C_n^2 based on temperature conditions. At the end of this work, a regression model is proposed that can be used in scenarios over flooded areas to obtain nocturnal turbulence, if the climatic parameters are available.

To achieve this goal, this work is organized as follows. Section 2 provides the theoretical background behind the FSO and its performance under atmospheric turbulence. Section 3 describes our experimental setup, used as a proof of concept. Section 4 analyzes the results. Finally, Section 5 presents the conclusion.

2. FSO LINKS UNDER ATMOSPHERIC TURBULENCE

Most optical communication systems use beams whose radiation profile can be modeled as Gaussian. This model is directly related to one of the most important wave solutions for the Helmholtz paraxial equation, which considers the fundamental mode of propagation (TEM₀₀), when the beams are originated by lasers or LEDs [23,24]. For a circular Gaussian beam propagating along free space, disregarding losses, the optical power intensity can be observed through the irradiance profile I , using a cylindrical coordinate system (ρ, ϕ, z) , given by [25]

$$I(\rho, \phi, z) = A_0^2 \frac{r_t^2}{r_L^2(z)} \exp\left[-\frac{2\rho^2}{r_L^2(z)}\right], \quad (1)$$

where A_0 is a constant related to the beam energy, r_t is the radius of the transmitter, and r_L is the radius of the beam at the observed point z .

It is noted that the radius of the beam width r_L , also known as spot size, represents the distance from the center where the irradiance decreases $1/e^2$ of its maximum. A widely used

approximation is $r_L(z) = r_t + \frac{\theta z}{2}$, where θ is the angle of divergence of the beam [26].

The power leaving the transmitter (P_{tx}) can be written as [27]

$$P_{tx} = \int_0^\infty \int_0^{2\pi} I(\rho, \phi, z) \rho d\phi d\rho = \frac{A_0^2 r_t^2 \pi}{2}. \quad (2)$$

The received power (P_{rx}) depends on the link alignment, atmospheric attenuation, transceiver losses, atmospheric turbulence, and the receiver's geometry. In dB, it is obtained by [28]

$$P_{rx} = P_{tx} + \alpha_{geo} + \alpha_{atm} + \alpha_{sci} + \alpha_{TR}, \quad (3)$$

where α_{geo} is the geometric and misalignment attenuation, α_{atm} is atmospheric attenuation, α_{sci} is scintillation attenuation, and α_{TR} are losses in the fiber-telescope interface of both transceivers. Usually, this loss ranges from 1 to 2 dB for each transceiver.

Every FSO link is subject to geometric attenuation. Due to diffraction, the beam will expand into the atmosphere and some of the energy will not be detected by the receiver. If there is misalignment, there will be even more attenuation. The geometric and misalignment attenuation of a circular Gaussian beam can be given as [25]

$$\alpha_{geo} = -10 \log \left[1 - Q_1 \left(\frac{2d}{r_L}, \frac{2r_r}{r_L} \right) \right], \quad (4)$$

where d is the total misalignment, r_r is the receiver aperture radius, and Q_1 is the first order Marcum Q-function.

Atmospheric attenuation depends on absorption and scattering caused by particles that are suspended in the air. A very simple and widely used model in the literature is to make [29]

$$\alpha_{atm} = 10 \log(\tau_a + \tau_b), \quad (5)$$

where τ_a and τ_b are the transmittances related to absorption and scattering, respectively. τ_a can be written as [29]

$$\begin{cases} \tau_a = \exp(-A_i \cdot \sqrt{w_a}), & \text{if } w_a < w_i, \\ \tau_a = k_i \cdot \left(\frac{w_i}{w_a}\right)^{\beta_i}, & \text{if } w_a > w_i, \end{cases} \quad (6)$$

where A_i , k_i , β_i , and w_i are constants tabled in [29], and w_a is a water precipitation measure. τ_b can be written as [10]

$$\tau_b = \exp\left\{-L \cdot \left[\frac{3,912}{V} (550)^\delta \cdot \lambda^{-\delta} + C_2 \cdot \lambda^{-4}\right]\right\}, \quad (7)$$

where, typically, $C_2 = 0.00258$, V is the air visibility in km, L is the length of the link, and δ is the size distribution coefficient of scattering, which can be determined by Kim's model [10]. Depending on the local weather conditions, an extra term can be included to represent attenuation by rain, snow, or smoke [8,9,30].

A. Atmospheric Turbulence

Scintillation attenuation is a direct consequence of atmospheric turbulence. The atmosphere is a very complex fluid, with variations in temperature and pressure at different points. Due to these gradients between the surface and the atmosphere, air pockets with different refractive indices are formed. These

small air pockets act as prisms, causing deflection and eventually constructive or destructive interference. Atmospheric turbulence is a random phenomenon that represents the level of heterogeneity of this fluid. In addition to temperature and pressure, the refractive index of air depends on the wavelength, humidity, and molecular composition of the air. For the FSO range of interest, random variations in temperature and pressure are much more relevant. Thus, the refractive index at a point R can be written according to Eq. (8). However, as atmospheric pressure variations are normally very small, the temperature becomes the main factor for the refractive index characterization [8,11,31]:

$$n(R) \approx 1 + 79 \cdot 10^{-6} \frac{P(R)}{T(R)}, \quad (8)$$

where n is the refractive index, P is the pressure in hPa, and T is the air temperature in K.

To deal with this random characteristic of air in relation to temperature, a statistical approach is needed. This approach has its origins in Kolmogorov's classical theory of turbulence, developed in the 1940s to study fluctuations in the velocity of a fluid. According to this theory, a turbulent fluid has coherent structures of vortices or eddies of different sizes, where there is a transfer of energy from the larger ones (macro-scale L_0) to the smaller ones (micro-scale l_0) in a cascade effect. These ideas were used to also characterize scalar quantities, such as temperature variations. Considering these homogeneous and isotropic fluctuations, it is possible to write a structural function for the temperature distribution. As the refractive index is related to temperature through Eq. (8), it is also possible to write a structural function and define a structural constant for the refractive index [11].

The refractive index can be written as a random field in space in the form $n(R) = 1 + n_1(R)$, where n_1 is a null-mean random variable that represents variations in the index. Considering the homogeneous and isotropic field, the covariance function of n_1 is dependent only on the scalar distance between two points in space ($R = |R_1 - R_2|$). Thus, the structural function becomes [11]

$$D_n(R) = 2 [B_n(0) - B_n(R)] = \begin{cases} C_n^2 R^{2/3}, & l_0 \ll R \ll L_0 \\ C_n^2 l_0^{-4/3} R^2, & R \ll l_0 \end{cases}, \quad (9)$$

where B_n is the covariance function of n , the limits l_0 and L_0 represent the scale range for the turbulent eddies, where it is valid for homogeneous and isotropic media. The refractive index structure constant C_n^2 , also known as the structural parameter, is the most important parameter in the classification of a turbulent atmosphere. This parameter can be estimated using one of several models or measured using a scintillometer [8].

The fact that the refractive index is a random variable leads us to seek a solution to the stochastic Helmholtz equation. As a closed solution for this equation is not yet known, two approximate and limited approaches, known as Born and Rytov approximations, have been proposed. By statistically analyzing both solutions, through the modeling of their moments up to the fourth order, it can be seen that the irradiance profile of a beam propagating along the turbulent channel suffers a series

of distortions in relation to Eq. (1). It is worth highlighting the three main negative effects of atmospheric turbulence: beam scintillation, beam wander, and beam spreading [11].

Beam wander can be interpreted as the random occurrence of small angular deviations of the beam in the receiving plane. These deviations generate a wandering movement in relation to the reference center. Thus, beam wander is characterized by the variance of these deviations from the center. In beam spreading, there is a relative increase in the divergence of the beam. It is common to build a model based on long- and short-term observations. When computing long-term wandering and spreading motions, the expected value for the beam radius is greater than the radius without turbulence effects. These movements are related by [31]

$$W_{LT} = \sqrt{W_{ST}^2 + \langle r_c^2 \rangle}, \quad (10)$$

where W_{LT} is the long-term radius, W_{ST} is the short-term radius (instantaneous widening), and $\langle r_c^2 \rangle$ is the variance of beam deviation.

The beam wander variance ($\langle r_c^2 \rangle$) and the structural parameter of the refractive index have an empirical relationship [Eq. (11)], which is suitable for weak and intermediate turbulence [11]:

$$\langle r_c^2 \rangle = 2.42 C_n^2 L^3 W^{-1/3}, \quad (11)$$

where $W = \frac{r_f}{\sqrt{2}}$.

However, the main consequence of turbulence to link performance is the scintillation effect. Scintillation causes the receiver to detect temporal or spatial variations in the beam's irradiance profile and, consequently, in the received power. This means that the irradiance profile, in reality, is a random variable represented by a probability distribution function, such as log-normal, gamma-gamma, I-K, Exp. Weibull, M, among others. In practice, when making a link power budget, we can work with the concept of equivalent scintillation attenuation. Some simplified models propose deterministic approximations for this quantity [32–34]. More accurate results for calculating this parameter for specific cases are presented in [12].

B. Method for Measuring C_n^2

To compute the equivalent scintillation attenuation, some knowledge of C_n^2 is required. Andrews and Phillips [11] propose a very low-cost technique for measuring C_n^2 based on atmospheric parameters. For Kolmogorov turbulence, they define the temperature structure constant C_T^2 and the refractive index structure constant C_n^2 as, respectively [11],

$$C_T^2 = \langle [T(\vec{x}) - T(\vec{x} + \vec{r})]^2 \rangle r^{-2/3}, \quad l_0 \leq r \leq L_0, \quad (12)$$

$$C_n^2 = \langle [n(\vec{x}) - n(\vec{x} + \vec{r})]^2 \rangle r^{-2/3}, \quad l_0 \leq r \leq L_0, \quad (13)$$

where the symbol $\langle \cdot \rangle$ denotes an ensemble average, T is the atmospheric temperature in K, n is the refractive index, \vec{x} and \vec{r} are spatial position vectors, and r is the amplitude of \vec{r} .

The relationship between the temperature structure constant C_T^2 and the refractive index structure constant C_n^2 is expressed as [11,35]

$$C_n^2 = \left(79 \times 10^{-6} \frac{P}{T^2}\right) C_T^2, \quad (14)$$

where P is the atmospheric pressure in hPa.

3. EXPERIMENTAL SETUP

As a proof of concept for the proposed method, we were inspired by a typical scenario of the Amazon region, where the link could connect two points on opposite banks over a large river. In this scenario, there is great heterogeneity in the medium, as part of the link will be over water and part over land. Thus, we designed a reduced experimental setup simulating this scenario. An outdoor FSO link was established, 70 cm above a pool, as can be seen in Fig. 1.

Nine days of experiments were carried out at night. All experiments had a link length, L , of 4.5 m. However, for each day, the length of the link over water, w , was varied. Table 1 presents, in the second column, the ratio between the length of water and the length of link, w/L , for each test performed, as well as, for the other columns, the range of daily variation of some atmospheric parameters, such as air temperature (T_{air}), water–air temperature difference (Dif), relative humidity (RH), pressure (P), and dew point (DP).

To measure the temperature and relative humidity of the environment, four AM2302 DHT22 sensors, from the manufacturer Aosong (Guangzhou) Electronics Co., were used along the link. The link humidity was calculated by the arithmetic mean of the four measurements. However, to calculate the value of C_n^2 using the method presented in Section 2.B, only the temperature measurements of the sensors located at the ends of the link were used. During all experiments, the water

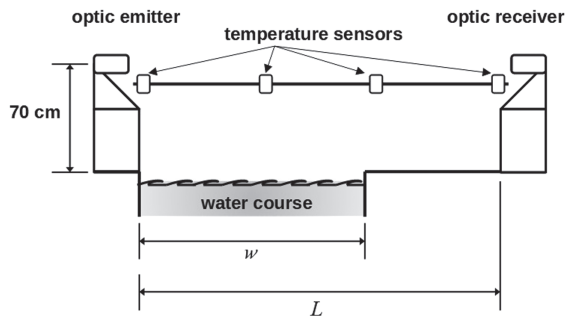


Fig. 1. Experimental setup for measuring C_n^2 in an FSO transmission over water.

temperature was also measured, using a DS18B20 sensor, from the manufacturer Dallas Semiconductor.

All sensor data were collected using an Arduino UNO and were processed in MATLAB R2002a software. Other atmospheric parameters, such as dew point and atmospheric pressure, were collected from the meteorological station at Jacarepaguá airport, located 2.5 km from the place where the experiments were carried out.

In the experimental setup, a real transmitter was used. An optical telescope, consisting of a circular plano–convex lens with a radius of 2.1 cm, was built by our team. The optical source was a 980 nm pump laser with a power of 15.3 dBm. Due to the link distance, the source was attenuated to -10 dBm using a variable attenuator.

Using the method presented in Section 2.B to correctly measure turbulence, it is possible to define statistical models of C_n^2 using meteorological data. As input to the model, we will consider the air temperature and atmospheric pressure, according to Eq. (8), plus other parameters that will depend on the scenario. The next section presents a proof of concept and its results.

4. RESULTS AND DISCUSSION

The first test was carried out with the length of the link completely over water. It is common to have a large temperature difference between rivers and the air in the Amazon region. Hence, we decided to analyze the influence of this temperature difference on the C_n^2 measurements. The average air temperature was colder than the water. Figure 2 presents the result for the $\log(C_n^2)$ over time. On the right vertical axis, it is also possible to verify the temperature difference between water and air over time. A strong positive correlation between the $\log(C_n^2)$ and the temperature difference can be noted. These results are in agreement with [15,36], where strong positive correlations between these two parameters are also found, which confirms the strong influence of the temperature difference between water and air on atmospheric turbulence.

We believe a strong turbulence profile was obtained due to the differences in terrain (water and ground), which maximize the temperature differences (water, ground, and air), especially after sunset, when temperature inversion between water and air occurs.

For the statistical modeling of an FSO link over the sea, some atmospheric parameters are commonly used as input parameters. In Lionis *et al.* [14], these parameters are: air temperature (T_{air}), pressure (P), dew point (DP), relative humidity (RH),

Table 1. Conditions of the Experimental Tests

Trial	w/L	T_{air} (K)	Dif (°C)	RH (%)	P (hPa)	DP (°C)
1	1.0	290.89–292.23	3.90–5.46	70–81	1019	13
2	0.8	291.68–295.05	1.72–4.66	65–84	1017	16
3	0.7	295.48–297.84	−0.02–2.51	73–87	1007–1009	21
4	0.6	294.25–298.95	1.39–4.71	77–99	1014–1016	19
5	0.5	292.55–296.95	3.01–6.85	65–83	1019–1021	21.00
7	0.4	293.35–296.95	1.76–4.92	76–94	1014	19
6	0.4	293.64–296.95	3.67–6.25	74–89	1011–1014	21
8	0.3	293.08–294.53	3.86–4.99	64–88	1022	15
9	0.2	293.35–296.95	1.76–4.92	76–94	1013–1015	21

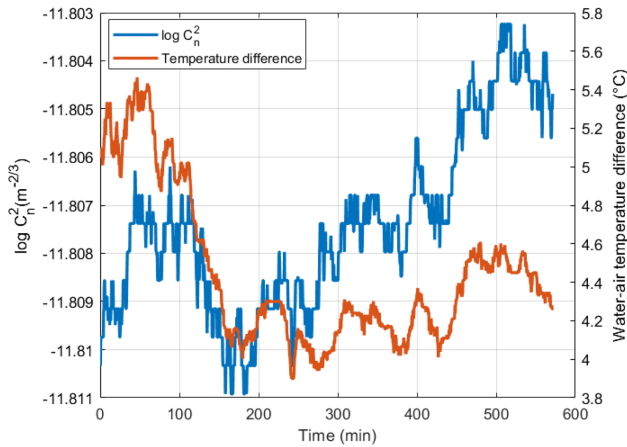


Fig. 2. C_n^2 and water–air temperature difference over time.

wind speed (WS), and solar radiation (SF). In our model, we did not consider WS or SF , since the experiments were carried out at night and in an environment where the wind was measured as null. However, our first test showed that the scenario would be better characterized if we also considered the temperature difference between water and air. Thus, this temperature difference was also used as an input parameter and named Dif . Furthermore, the width of the river (w) and the total length of the link (L) were also considered. It was decided to include these two parameters as the relation w/L . Having these input parameters and using the method of Section 2.B to calculate C_n^2 as output, a prediction model can be obtained, such as the one presented in Fig. 3.

The data collection was made for almost 3 months. Nine trials were performed for different wet section lengths and fixed link lengths. Most tests ran in 10 h each; only one ran in 5 h. Measurements of T_{air} , Dif , and RH were taken from sensors at the experiment site. Measures of DP and P were taken at a nearby meteorological station. The way in which atmospheric parameters were collected on each day was identical for each test day. The ranges of values for each environmental parameter are presented in Table 2.

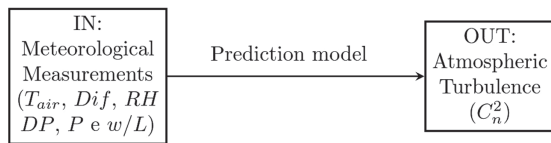


Fig. 3. Modeling of the system to predict C_n^2 in heterogeneous scenarios.

Table 2. Atmospheric Parameter Values

Parameter	Min. Value	Mean Value	Max. Value
T_{air} (K)	290.89	294.48	298.95
Dif (°C)	-0.02	3.86	6.85
RH (%)	65	79.91	99
P (hPa)	1007	1015.25	1021
DP (°C)	13	18.5	21
w/L	0.2	0.59	1
$\log(C_n^2)$	-12.41	-11.89	-11.66

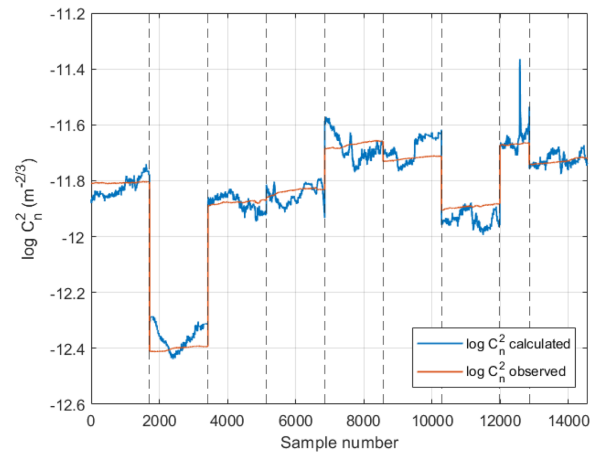


Fig. 4. Comparison of the calculated and observed $\log(C_n^2)$ for the nine test days.

The expression given by Eq. (15) can be used in any region, as long as the atmospheric parameters have values close to those represented in Table 2 and that the measurements of C_n^2 are over water.

A. C_n^2 Statistical Modeling

From the data collected during this experimental procedure, a second-order prediction model for $\log(C_n^2)$ was built, using the least squares method. Our regression presented an R-squared parameter value of 0.955982, which represents a great similarity between the measured and predicted values. The resulting regression model is given as

$$\begin{aligned}
 \log(C_n^2) &= 225.711 - 1.704 \cdot T_{air} + 3.01 \times 10^{-3} \cdot T_{air}^2 \\
 &\quad - 9.544 \times 10^{-3} \cdot RH + 1.536 \times 10^{-4} \cdot RH^2 \\
 &\quad - 4.012 \times 10^{-2} \cdot Dif + 6.642 \times 10^{-3} \cdot Dif^2 \\
 &\quad + 1.866 \times 10^{-2} \cdot P - 1.820 \cdot DP + 4.976 \times 10^{-2} \cdot DP^2 \\
 &\quad + 2.249 \cdot (w/L) - 2.737 \cdot (w/L)^2.
 \end{aligned} \tag{15}$$

Aiming to compare the built model (blue line) with the measured values (red line) of $\log(C_n^2)$, the data from all test days are plotted in Fig. 4.

The eighth day of testing was performed in a shorter time, but this fact did not interfere with the construction of Eq. (15). In this comparison, the RMSE is 0.044822 and the maximum error is 2.58% of the observed $\log(C_n^2)$, which represents a very satisfactory result.

It is interesting to observe the isolated behavior of two important parameters of this modeling. In Fig. 5(a), it is possible to verify the variation of $\log(C_n^2)$ in relation to Dif , considering six measures of w/L and average parameters of T_{air} , P , RH , and DP . The curves have the expected behavior, according to the literature [36]. In Fig. 5(b), it is possible to verify the variation of $\log(C_n^2)$ as a function of w/L , considering four

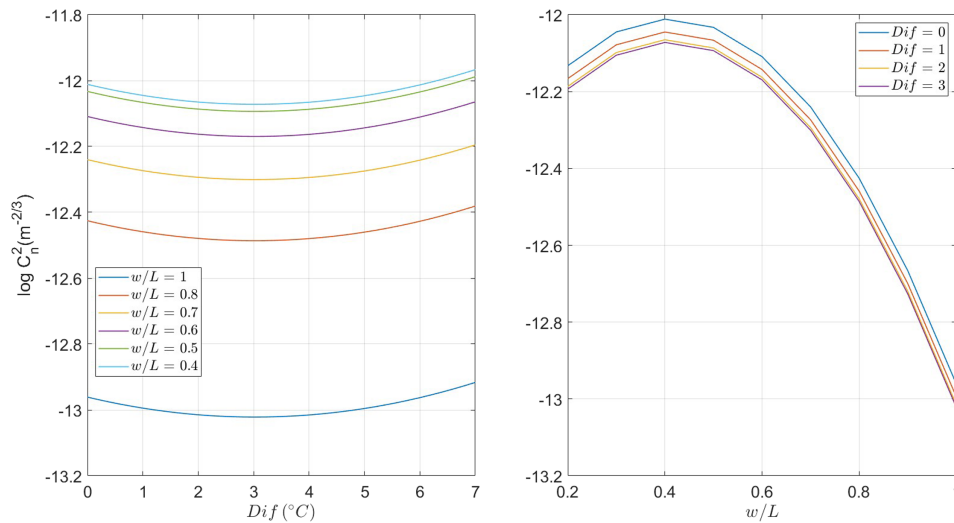


Fig. 5. Effects of Dif and w/L on turbulence.

measures of Dif and average values of the other atmospheric parameters described above. The relation w/L presents a particularly interesting and intuitive effect, in which the $\log(C_n^2)$ is maximized when w is 40% of L , i.e., a proportion close to a scenario as heterogeneous as possible. This last finding confirms the assumption that the watercourse will negatively affect the performance of the link, especially if there is a link proportion of approximately 40% between river and land.

In [15], an FSO link was established at 35 m above the water level; the correlation between the value of C_n^2 obtained by Eq. (15) and the RSSI value obtained in [15] was -0.91 on average, considering all test days. This fact leads to the conclusion that the method provided by Eq. (15) can also work at a height of 35 m above sea level.

Although the values found from Eq. (15) are high when compared with the values of methods established in the literature, it is important to emphasize the high correlation between the vectors obtained by Eq. (15) and the RSSI values obtained by the method found in [15], $R^2 = 0.7$. This fact shows that the model proposed here is capable of providing the behavioral variations of the C_n^2 curve over time.

5. CONCLUSIONS

In this paper, a low-cost methodology for measuring the structural parameter of the refractive index was presented. This parameter allows the use of simple models to describe the influence of atmospheric turbulence on the performance of an FSO link. With this information, it is possible to carry out a much more complete power balance, even in very heterogeneous scenarios, where the construction of an analytical model would be very difficult. It was possible to verify the negative impact of watercourses on the performance of an FSO link. Conditions of a temperature difference between water and air above 3°C , in addition to a relationship close to 40% between link length and river width, act as maximizers of turbulence.

Through these procedures, it was also possible to build and validate an empirical model, based on meteorological measurements performed in an outdoor environment. This low-cost

methodology can be used in the most diverse scenarios, whether in a controlled environment or an external environment.

Disclosures. The authors declare no conflicts of interest.

Data availability. Data underlying the results presented in this paper are not publicly available at this time but may be obtained from the authors upon reasonable request.

REFERENCES

1. Instituto Brasileiro de Geografia e Estatística, "Cidades e Estados," <https://www.ibge.gov.br/cidades-e-estados/am/sao-gabriel-da-cachoeira.html>.
2. J. Wagner, Minister of State for Defense Ricardo Berzoini, Minister of State for Communications, and Aldo Rebelo, Minister of State for Science, Technology and Innovation, "Portaria Interministerial N° 586 de 22 de junho de 2015," http://www.amazoniaconectada.eb.mil.br/images/manuais/DOU_2015_07_Seca_1_pdf_20150723_25_Portaria_Interministerial_Amazonia_Conectada.pdf.
3. Comando Militar da Amazônia, "Projeto Amazônia Conectada," <http://www.amazoniaconectada.eb.mil.br/ultimas-noticias-na-midia/93-projeto-amazonia-conectada-e-lancado-no-municipio-de-sao-gabriel-da-cachoeira-am>.
4. D. Kedar and S. Arnon, "Urban optical wireless communication networks: the main challenges and possible solutions," *IEEE Commun. Mag.* **42**, S2–S7 (2004).
5. A. B. Raj and A. K. Majumder, "Historical perspective of free space optical communications: from the early dates to today's developments," *IET Commun.* **13**, 2405–2419 (2019).
6. Y. Ren, Z. Wang, P. Liao, L. Li, G. Xie, H. Huang, Z. Zhao, Y. Yan, N. Ahmed, M. P. J. Lavery, N. Ashrai, S. Ashrafi, R. D. Linquist, M. Tur, I. B. Djordjevic, M. A. Neifeld, and A. E. Willner, "400-Gbit/s free-space optical communications link over 120-meter using multiplexing of 4 collocated orbital-angular-momentum beams," in *Optical Fiber Communication Conference (OSA, 2015)*, paper M2F.1.
7. T. R. Raddo, S. Rommel, B. Cimoli, C. Vagionas, D. Perez-Galacho, E. Pikasis, E. Grivas, K. Ntontin, M. Katsikis, D. Kritharidis, E. Ruggeri, I. Spaleniak, M. Dubov, D. Klonidis, G. Kalfas, S. Sales, N. Pleros, and I. T. Monroy, "Transition technologies towards 6G networks," *EURASIP J. Wireless Commun. Netw.* **2021**, 100 (2021).
8. H. Kaushal and G. Kaddoum, "Optical communication in space: challenges and mitigation techniques," *Commun. Survey Tuts.* **19**, 57–96 (2017).
9. ITU-R, "Propagation data required for the design of terrestrial free-space optical links," Recommendation P.1817-1 (2012).

10. I. I. Kim, B. McArthur, and E. J. Korevaar, "Comparison of laser beam propagation at 785 nm and 1550 nm in fog and haze for optical wireless communications," *Proc. SPIE* **4214**, 26–37 (2001).
11. L. C. Andrews and R. L. Phillips, *Laser Beam Propagation through Random Media*, 2nd ed. (SPIE, 2005).
12. G. K. Rodrigues, V. G. A. Carneiro, A. R. da Cruz, and M. T. M. Giraldi, "Evaluation of the strong turbulence impact over free-space optical links," *Opt. Commun.* **305**, 42–47 (2013).
13. J. Latal, J. Vitasek, L. Hajek, A. Vanderka, P. Koudelka, S. Kepak, and V. Vasinek, "Regression models utilization for RSSI prediction of professional FSO link with regards to atmosphere phenomena," in *International Conference on Broadband Communications for Next Generation Networks and Multimedia Applications (CoBCom)* (2016), pp. 1–6.
14. A. Lionis, K. Peppas, H. E. Nistazakis, A. D. Tsigopoulos, and K. Cohn, "Experimental performance analysis of an optical communication channel over maritime environment," *Electronics* **9**, 1109 (2020).
15. A. Lionis, K. Peppas, H. E. Nistazakis, A. Tsigopoulos, and K. Cohn, "Statistical modeling of received signal strength for an FSO link over maritime environment," *Opt. Commun.* **489**, 126858 (2021).
16. D. Sadot and N. S. Kopeika, "Forecasting optical turbulence strength on the basis of macroscale meteorology and aerosols: models and validation," *Opt. Eng.* **31**, 200–212 (1992).
17. Y. Jiang, J. Ma, L. Tan, S. Yu, and W. Du, "Measurement of optical intensity fluctuation over an 11.8 km turbulent path," *Opt. Express* **16**, 6963–6973 (2008).
18. L. Yatcheva, R. Barros, M. Segel, D. Sprung, E. Sucher, C. Eisele, and S. Gladysz, "Ultimate turbulence experiment: simultaneous measurements of C_n^2 near the ground using six devices and eight methods," *Proc. SPIE* **9641**, 964105 (2015).
19. V. N. H. Silva, A. P. L. Barbero, and R. M. Ribeiro, "A new triangulation-like technique for the evaluation of the refractive index structure constant C_n^2 in free-space optical links," *J. Lightwave Technol.* **29**, 3603–3610 (2011).
20. J. Svoboda, Z. Chladova, P. Pesice, and O. Fiser, "FSO link attenuation and structure index derived from 3D sonic anemometer measurement," in *Proceedings of the 11th International Conference on Telecommunications (IEEE, 2011)*, pp. 219–222.
21. S. H. Jaber and M. H. Al-Jiboori, "Characteristics of $c_{\mu 2}$ derived from ultrasonic anemometer in an urban boundary layer," *Sci. Rev. Eng. Environ. Stud.* **28**, 14–24 (2019).
22. E. Polnau, D. L. N. Hettiarachchi, and M. A. Vorontsov, "Electro-optical sensors for atmospheric turbulence strength characterization with embedded edge AI processing of scintillation patterns," *Photonics* **9**, 789 (2022).
23. H. Kogelnik and T. Li, "Laser beams and resonators," *Appl. Opt.* **5**, 1550–1567 (1966).
24. B. E. A. Saleh and M. C. Teich, *Fundamentals of Photonics*, 3rd ed., Wiley Series in Pure and Applied Optics (Wiley, 2019).
25. C. P. Azzolin, A. F. Gurgel, and V. G. A. Carneiro, "Marcum Q-function as an analytical solution for misaligned Gaussian beams," *Opt. Eng.* **60**, 056105 (2021).
26. S. Bloom, E. Korevaar, J. Schuster, and H. Willebrand, "Understanding the performance of free-space optics [Invited]," *J. Opt. Netw.* **2**, 178–200 (2003).
27. J. Poliak, P. Pezzei, E. Leitgeb, and O. Wilfert, "Analytical expression of FSO link misalignments considering Gaussian beam," in *Proceedings of the European Conference on Network and Optical Communications (NOC), Optical Cabling and Infrastructure (OC&I)* (2013), pp. 99–104.
28. V. G. A. Carneiro, "CDMA óptico sobre óptica no espaço livre para comunicações móveis em sistemas de defesa," Ph.D. thesis (Instituto Militar de Engenharia, 2013).
29. D. Forin, G. Incerti, G. Tosi, A. Teixeira, L. Costa, P. D. Brito Andre, B. Geiger, E. Leitgeb, and F. Nadeem, *Free Space Optical Technologies* (InTech, 2010), pp. 257–296.
30. A. A. Basahel, M. R. Islam, S. A. Zabidi, and M. H. Habaebi, "Availability assessment of free-space-optics links with rain data from tropical climates," *J. Lightwave Technol.* **35**, 4282–4288 (2017).
31. L. C. Andrews, R. L. Phillips, C. Y. Hopen, and M. A. Al-Habash, "Theory of optical scintillation," *J. Opt. Soc. Am. A* **16**, 1417–1429 (1999).
32. L. Dordová and O. Wilfert, "Calculation and comparison of turbulence attenuation by different methods," *Radioengineering* **19**, 162–167 (2010).
33. O. Wilfert and Z. Kolka, "Statistical model of free-space optical data link," *Proc. SPIE* **5550**, 203–213 (2004).
34. J. A. H. Osório, "Simulação e desenvolvimento de um enlace de Free-Space Optics no Rio de Janeiro e a relação com a ITU-T G.826," Ph.D. thesis (Pontifícia Universidade Católica do Rio de Janeiro, 2005).
35. Y. Li, W. Zhu, X. Wu, and R. Rao, "Equivalent refractive-index structure constant of non-Kolmogorov turbulence," *Opt. Express* **23**, 23004–23012 (2015).
36. P. Frederickson, K. Davidson, C. Zeisse, and C. Bendall, "Estimating the refractive index structure parameter over the ocean using bulk methods," *J. Appl. Meteorol.* **39**, 1770–1783 (2000).